

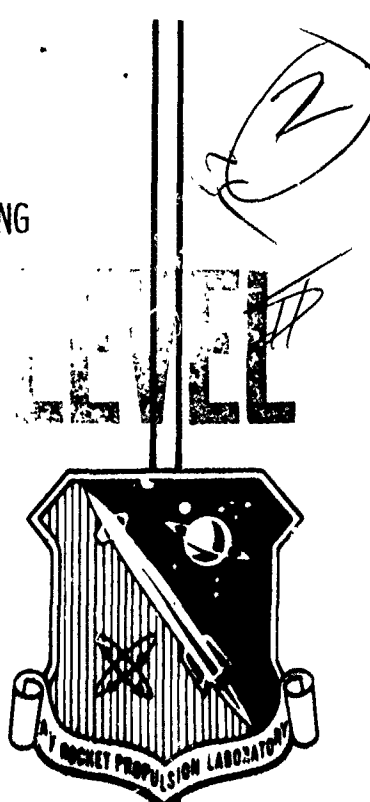
DA078904

AN INVESTIGATION OF PARTICLE SIZE DISTRIBUTION USING  
LASER HOLOGRAPHY OF BURNING SOLID PROPELLANT

AIR FORCE ROCKET PROPULSION LABORATORY  
EDWARDS AFB, CALIFORNIA 93523

AUTHORS: MICHAEL J. ADAMS  
T. W. OWENS

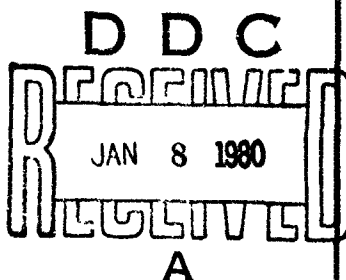
SEPTEMBER 1979



Approved for Public Release  
Distribution Unlimited

DDC FILE COPY

AIR FORCE ROCKET PROPULSION LABORATORY  
DIRECTOR OF SCIENCE AND TECHNOLOGY  
AIR FORCE SYSTEMS COMMAND  
EDWARDS AFB, CALIFORNIA 93523



80 1 7 179

## NOTICES

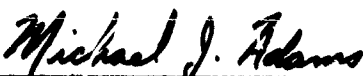
When U.S. Government drawings, specifications, or other data are used for any purpose other than a definitely related Government procurement operation, the Government thereby incurs no responsibility nor any obligation whatsoever, and the fact that the Government may have formulated, furnished, or in any way supplied the said drawings, specifications, or other data is not to be regarded, by implication or otherwise, as in any manner licensing the holder or any other person or corporation, or conveying any rights or permission to manufacture, use, or sell any patented invention that may in any way be related thereto.

## FOREWORD

This is a final report on research conducted in-house in the combustion technology section, Combustion and Plume Branch, Propulsion Analysis Division of the Air Force Rocket Propulsion Laboratory. The work was accomplished under the AFRPL project number 2308MICF. Work started in November 1977, and was terminated on 30 September 1978 due to technical problems.

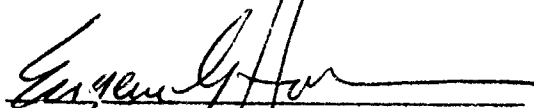
The authors would like to extend their sincere appreciation for the assistance given to them by Mr. Leon Triplett and Mr. David Cooke in the establishment of the holographic recording and reconstruction test areas.

This report has been reviewed by the Information Office/XOJ and is releasable to the National Technical Information Service (NTIS). At NTIS it will be available to the general public, including foreign nations. This technical report has been reviewed and is approved for publication; it is unclassified and suitable for general public release.



MICHAEL J. ADAMS  
Principle Investigator

FOR THE COMMANDER



EUGENE G. HABERMAN  
Chief, Propulsion and Analysis Division



WILBUR C. ANDREPONT  
Chief, Combustion Technology Section

## UNCLASSIFIED

SECURITY CLASSIFICATION OF THIS PAGE (When Data Entered)

REPORT DOCUMENTATION PAGE		READ INSTRUCTIONS BEFORE COMPLETING FORM
1. REPORT NUMBER <b>(14) AFRPL-TR-79-48</b>	2. GOVT ACCESSION NO.	3. RECIPIENT'S CATALOG NUMBER <b>(9)</b>
4. TITLE (and Subtitle) <b>AN INVESTIGATION OF PARTICLE SIZE DISTRIBUTION USING LASER HOLOGRAPHY OF BURNING SOLID PROPELLANT</b>		5. TYPE OF REPORT & PERIOD COVERED <b>FINAL REPORT, NOV 1977 - 30 Sep 78</b>
		6. PERFORMING ORG. REPORT NUMBER
7. AUTHOR(S) <b>Michael J. ADAMS T. W. OWENS</b>		8. CONTRACT OR GRANT NUMBER
9. PERFORMING ORGANIZATION NAME AND ADDRESS <b>AIR FORCE ROCKET PROPULSION LABORATORY/PACC EDWARDS AFB, CALIFORNIA 93523</b>		10. PROGRAM ELEMENT, PROJECT, TASK AREA & WORK UNIT NUMBERS <b>62302F 23084ICF (11) MI</b>
11. CONTROLLING OFFICE NAME AND ADDRESS <b>(12) 43</b>		12. REPORT DATE <b>SEP 1979</b>
14. MONITORING AGENCY NAME & ADDRESS (if different from Controlling Office)		13. NUMBER OF PAGES <b>42 pages</b>
		15. SECURITY CLASS. (of this report) <b>UNCLASSIFIED</b>
		15a. DECLASSIFICATION/DOWNGRADING SCHEDULE
16. DISTRIBUTION STATEMENT (of this Report)  <b>APPROVED FOR PUBLIC RELEASE; DISTRIBUTION UNLIMITED</b>		
17. DISTRIBUTION STATEMENT (of the abstract entered in Block 20, if different from Report)		
18. SUPPLEMENTARY NOTES		
19. KEY WORDS (Continue on reverse side if necessary and identify by block number)  <b>COMBUSTION PARTICLE SIZE DISTRIBUTION HOLOGRAPHY</b>		
20. ABSTRACT (Continue on reverse side if necessary and identify by block number)  <b>A test area was modified to allow holographic recordings to be made of burning solid propellant samples as contained in a pressurized window bomb. A holographic reconstruction area was also established. An attempt was made to develop a semi-automated holographic data retrieval (HDR) system using existing AFRPL hardware. The purpose of the HDR system was to retrieve particle size and positions information in a</b>		

**UNCLASSIFIED**

SECURITY CLASSIFICATION OF THIS PAGE(When Data Entered)

timely manner from holographic reconstructions of the propellant combustion. Experiments with the HDR system revealed serious deficiencies in the areas of resolution and particle recognition. Since a primary goal of the program was to establish particle distribution correlations from holographically derived particle information, the present program has been inactivated pending the development and acquisition of an improved HDR system.

**UNCLASSIFIED**

SECURITY CLASSIFICATION OF THIS PAGE(When Data Entered)

## PREFACE

The objective of this study was to obtain the particle size distribution in the combustion field above a burning solid propellant using holography. This study also sought to identify the influence of propellant formulation on that particle size distribution and attempted to identify an appropriate statistical representation of the particle size distribution above the surface of a burning solid propellant.

The program was terminated prior to obtaining any useful particle count data. Experiments using holographic reconstructions of an AF-1951 resolution target revealed that an on-site electronic image analyzer, proposed as an automated data retrieval system, could not detect small particles ( $<50\mu\text{m}$ ) though the recorded holograms did provide good particle size resolution ( $<10\mu\text{m}$ ) when examined visually. Holographic recordings exhibit limited contrast for small objects. Electronic edge detection for small objects could not be achieved against the background noise inherent to a holographic recording. Hardware limitations in the data retrieval effort coupled to a time constraint on the study forced a temporary abandonment of the experimental program. Manual data retrieval, though possible, was not implemented since the process is tedious, questionable as to accuracy, and much too time consuming to gather sufficient data to formulate meaningful statistical models. This report documents the proposed experiment and the reason for its unsuccessful conclusion. It is hoped that the experiences and supporting material found in this report may prove useful to those initiating similar studies in the future.

## TABLE OF CONTENTS

<u>SECTION</u>	<u>PAGE</u>
1.0 INTRODUCTION	7
1.1 BACKGROUND	7
1.2 DEFINITIONS	7
1.3 PARTICLE SAMPLING	8
2.0 LASER DIAGNOSTICS IN PARTICLE MEASUREMENT	11
2.1 LASER DOPPLER	11
2.2 LASER HOLOGRAPHY	13
2.3 HOLOGRAPHIC IMAGE RESOLUTION	17
3.0 EXPERIMENTAL INVESTIGATION	17
3.1 EXPERIMENT AND APPLICATION	17
3.2 PROPELLANT TEST MATRIX	18
3.3 THE HOLOGRAPHY SYSTEM	19
4.0 EXPERIMENTAL PROCEDURES	25
4.1 IMAGE INTERROGATION	25
4.2 PARTICLE RECOGNITION	28
4.3 ELECTRONIC IMAGE ANALYSIS	29
5.0 RESULTS AND DISCUSSION	31
5.1 INITIAL INVESTIGATIONS	31
5.2 COMBUSTION HOLOGRAMS	32
5.3 POSITIONING	33
5.4 PARTICLE FOCUS	35
6.0 CONCLUSIONS AND RECOMMENDATIONS	37
6.1 CONCLUSIONS	37
6.2 RECOMMENDATIONS	38
REFERENCES	40

## LIST OF FIGURES

<u>FIGURE</u>		<u>PAGE</u>
1	PARTICLE SIZE MEASUREMENT: RESOLUTION	10
2	VELOCIMETER AND PARTICLE SIZING SCHEMATIC	12
3	RECORDING OF OFF-AXIS HOLOGRAMS	14
4	RECONSTRUCTION OF OFF-AXIS HOLOGRAMS	15
5	LAYOUT OF RECORDING AREA	22
6	LAYOUT OF RECONSTRUCTION AREA	23
7	LENS BOX ADJUSTMENT FIXTURE	24
8	SCENE INTERROGATION	26
9	ELECTRONIC PARTICLE DETECTION AND SIZING	30
10	FOCUS CRITERIA	36

LIST OF TABLES

<u>TABLE</u>		<u>PAGE</u>
1	LASER SPECIFICATIONS	20
2	PROPELLANT TEST MATRIX	21

## 1.0 INTRODUCTION

### 1.1 Background

1.1.1 Acoustic instabilities are often observed in solid rocket motors. Quite simply, instability occurs in a motor when the delicate balance between driving and damping mechanisms is sufficiently perturbed to allow finite pressure disturbances to grow (Reference 1). Logically, one can seek to suppress observed instability by decreasing driving or increasing damping within the motor cavity. Additives are introduced in the fuel to produce particles which are in turn ejected into the combustion flow field (Reference 2). The presence of solid particulate provides a mechanism to dissipate acoustic energy by increasing particle damping and decreasing driving mechanisms.

1.1.2 Theoretical observations indicate that optimal damping appears to be dependent on the size of the particles within the motor cavity (References 3 and 4). Optimal damping occurs when the dynamic and thermal relaxation times associated with the particles equals that of the acoustic period within the motor. Acoustic attenuation is therefore dependent on both frequency and particle size, and concentration.

1.1.3 Though particles assist in suppressing acoustic instability, particles also reduce motor performance. Theoretical investigations (Reference 5) have shown that the dynamic and thermal lags from the presence of particles can reduce expected thrust. Therefore, one must balance acoustic suppression against acceptable performance loss. Ideally, an optimum particle size is sought based upon this trade-off.

### 1.2 Definitions

1.2.1 Before proceeding with further discussion, it will be beneficial to provide clarification concerning some of the terminology to be used in this report. Unless stated otherwise, the term "particle" is used to identify any solid matter occupying the gaseous media above the surface of a burning solid propellant. No distinctions are made regarding the identity (i.e. composition) of particles. Although solid particles below 100 $\mu\text{m}$  are rarely spherical (Reference 6), references to particle size measurement shall imply

a spherical shape consideration.

1.2.2 One often refers to the dispersion of particles in a gaseous media. Dispersion constitutes the spread of particle size around a statistical mean. Monodispersed particles are of a single size, a situation quite rare in naturally occurring two-phase flow systems. Polydispersed particles show a distribution in size. Statistical methods are employed to simplify the representation of particle size in a polydispersed flow field. The combustion field above a burning solid propellant is an example of a polydispersed flow field. In this field, particles range in size from submicron to several hundred microns in diameter.

1.2.3 A particle count determines the frequency of occurrence of discrete particle sizes within a fixed volume. Particle counts are generally represented by a histogram. Given a sufficiently large particle count, the associated histogram can be smoothed to obtain a size frequency curve. Once normalized, the area between any interval on the abscissa to this curve defines the probability of finding a particle size within that interval.

1.2.4 Particle counts are used to obtain number-size distributions. Henceforth, the label size distribution shall imply equivalence to a number-size distribution. When a size distribution shows a single characteristic peak, the distribution is called unimodal. Unimodal distributions are labeled homogeneous. Size distributions showing several peaks are called multimodal and hence labeled heterogeneous.

1.2.5 Appropriate statistical definitions and considerations with regard to particle field analysis can be found in References 7 or 8. In general, the most common approach is to "fit" particle size data to well known statistical forms, for example, in log-normal distributions. Such distributions are well characterized and easily programmed into a theoretical study.

### 1.3 Particle Sampling

1.3.1 Various theoretical analyses can be applied to predict the effects of particle size distribution on stability and performance (References 3

through 5). These same methods can also be used in a parametric study to predict an optimum particle size distribution with regard to a particular motor/propellant combination. However, any theoretical prediction needs experimental verification. Unfortunately, it is not possible to cast propellants which will exhibit an a priori choice of particle size distribution in the combustion field. A more logical experiment is to obtain a particle size distribution measurement from subscale testing and then use that measurement in stability and performance analyses. Since particle distribution represents an empirically derived quantity, a particle count must be made by sampling the combustion flow field. Particle sampling is accomplished using physical or optical methods. An indication of size resolution which can be obtained using optical and physical methods is illustrated in Figure 1.

1.3.2 Physical sampling of a combustion flow field primarily uses collection devices to gather particles. For example, during propellant combustion, particles in the flow field are allowed to impact a holding material or quench liquid. The collected particles are then carefully distributed on slides. Size and count information are determined by electronic or mechanical sizing instrumentation. There are problems associated with particle collection. First, particle samples are gathered outside the combustion environment. Particle collection in a combustion flow field is quite difficult and also disturbs the flow structure. Second, the method of collection may physically alter the particles lending uncontrollable bias to any size distribution correlation. Third, once collected, the particles generally require careful preparation before size and count measurements are taken. All of the aforementioned problems lead one to try optical methods to sample particle laden flows.

1.3.3 In contrast to collection devices, optical methods do not gather physical objects. One does require that the flow be accessible to a light beam via windowing. Optical sampling does not interfere with the flow field and therefore permits sampling in the actual combustion environment. However, effects such as flame luminosity or high particle loading (i.e., concentration) may interfere with optical detection methods.

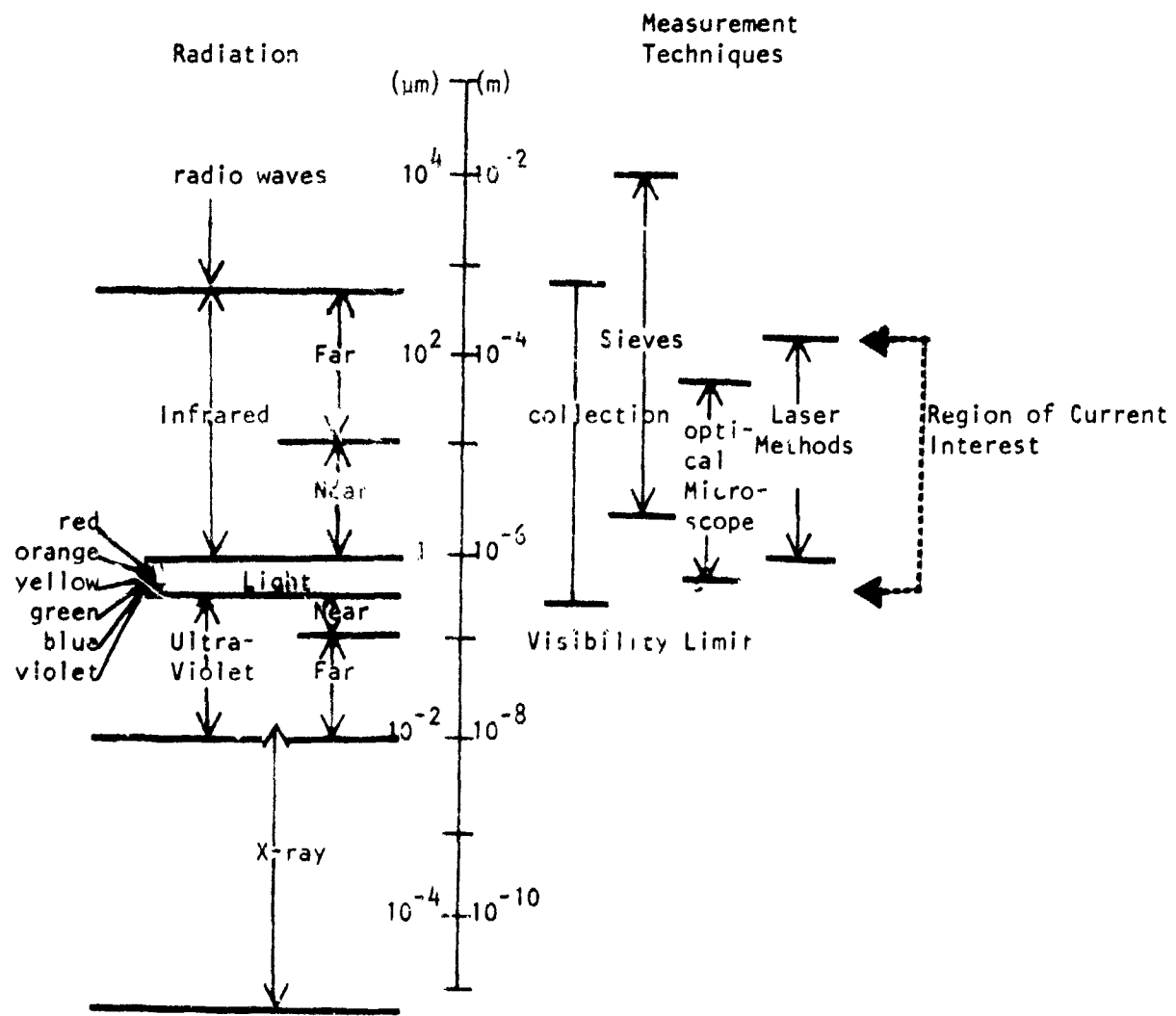


Figure 1. Particle Size Measurement: Resolution

1.3.4 There are several optical methods used in particle size measurement, two of which are laser doppler and laser holography. The first method constitutes a fixed point, real-time measurement while the latter method is a fixed time, spatial measurement.

## 2.0 LASER DIAGNOSTICS IN PARTICLE MEASUREMENT

### 2.1 Laser Dóppler

2.1.1 The key premise behind the use of a laser doppler system is that measurable properties of scattered light are dependent on the size and optical properties of the particles which scatter the light, i.e., illuminated particles serve as secondary radiation sources. A typical laser doppler arrangement is shown schematically in Figure 2. A laser source is divided into two spatially separated beams of equal intensity. The two beams are focused to some crossover point where they establish a fringe pattern of varying intensity. The fringe pattern fills a small ellipsoid volume and as such is viewed as a point measurement in the flow under examination. Particles in the combustion flow pass through the scene volume and disturb the fringe spacing. The scene volume is "observed" with one or more photodetectors. A disturbance in the scene volume is seen as a modulated signal from the photodetector. Signal modulation is examined with a pulse height analyzer to extract flow field information.

2.1.2 Particle size information is obtained from the visibility of the output signal from the photodetector (References 9 and 10). Visibility represents an average intensity value and is a measure of the extent to which the doppler frequency can be measured. Ideally, there exists a one-to-one linear relationship between measured light intensity and particle size. Light intensity is related to the depth of the modulated signal which in turn is represented by measured visibility. Durst and Eliasson (Reference 10) suggest an additional measurement of signal amplitude be made to establish particle size. A laser doppler derived size measurement in a poly-dispersed particle field is an average value. This average value can vary depending on the shape of the particles, particle concentration, and the size range of the particles.

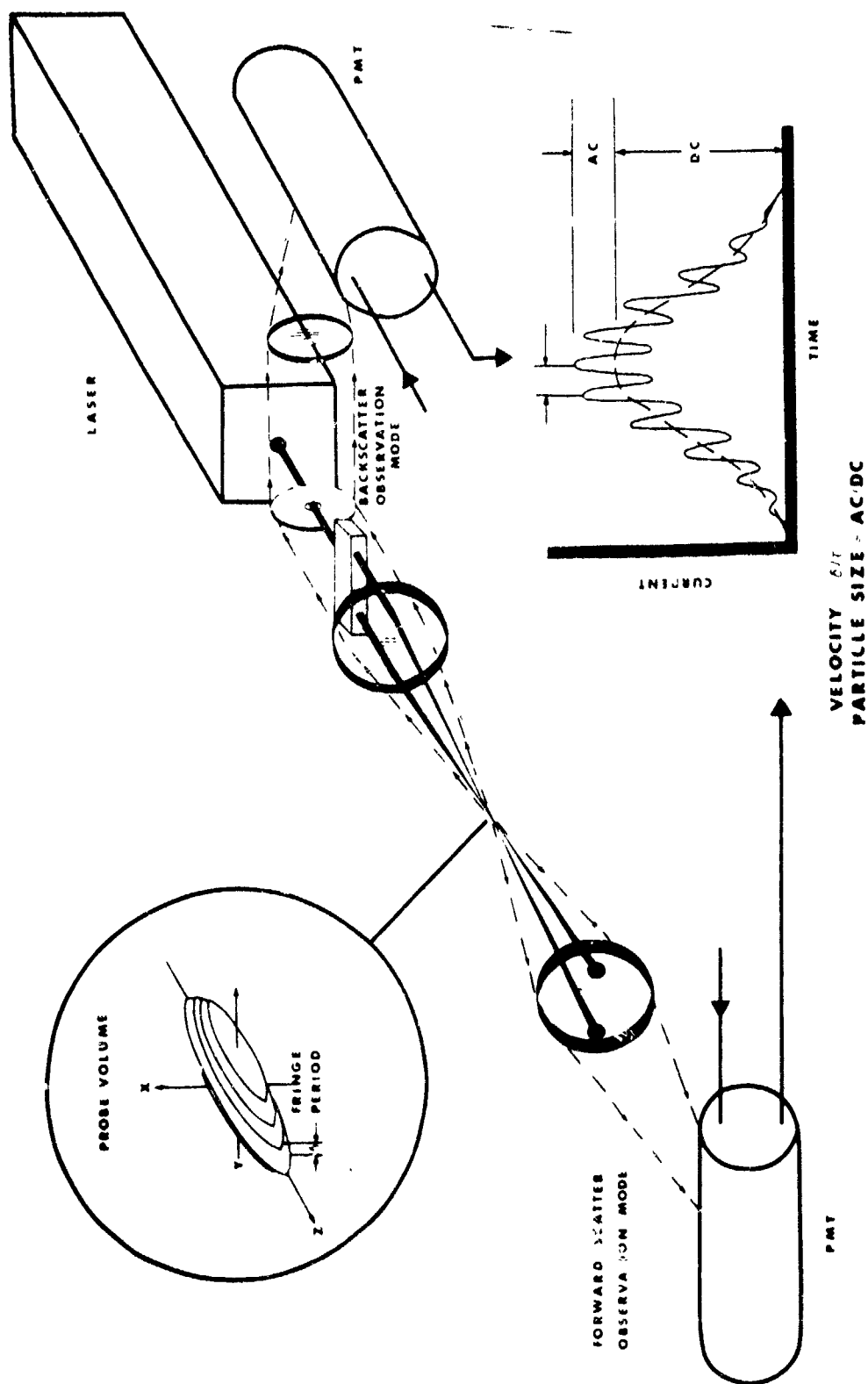


FIGURE 2. VELOCIMETER AND PARTICLE SIZING SYSTEM SCHEMATIC (COURTESY OF REFERENCE 10)

2.1.3 There are several limitations to extracting particle size information from a laser doppler apparatus. First, this method of size measurement requires careful calibration of the response of the system to establish the particle size range where the presupposed linear response assumption is valid. Second, if the intensity of a laser beam is assumed to be Gaussian, proper weighting must be applied to derive particle distributions to avoid biasing to larger particle sizes. Third, a high particle concentration can cause multiple scattering to occur which results in a saturated signal from the photodetector. This saturation limit is dependent upon the size of the particulate; however, a reasonable upper limit in combustion flows appears to be around  $10^4$  particles/cm<sup>3</sup>. Other effects such as flame luminosity can also interfere with the photodetector signal. A complete discussion of problems associated with doppler measurements can be found in Reference 9. The present study chose to use laser holography to obtain measurements of particle size and count.

## 2.2 Laser Holography

2.2.1 A photograph represents an instantaneous recording of a scene as projected two-dimensionally onto a light-sensitive material. Photographs are a record of the amplitude of an incident object wave from the scene. Amplitude information is realized as image contrast on the developed picture. A photograph exhibits limited depth of field and restricted viewing. For example, one cannot see behind objects recorded in the foreground. However, limited parallax can be obtained with stereoscopic methods.

2.2.2 A hologram also represents an instantaneous recording on light-sensitive material. However, unlike a conventional photograph, a hologram contains a record of both the amplitude and phase of the object wave which passes through the scene. The addition of phase information allows the scene to be reconstructed at any later time. Holograms give an extended depth of field that is many times greater than that exhibited by conventional photographs. The field of view in the recorded scene is limited primarily by the resolution capability of the recording material. One obtains virtually complete parallax in holographic recordings. By changing the observation point in a holographic reconstruction, one can see throughout the entire scene volume, hence in three dimensions.

2.2.3 Phase information is introduced to a holographic recording through a coherent reference wave with a known phase distribution. The reference wave acts as a carrier frequency to the object wave. The method one uses to introduce the reference wave into the recording distinguishes between two holographic techniques, namely in-line or off-axis recording. Further discussion will be restricted to the off-axis method shown schematically in Figures 3 and 4 (Reference 12).

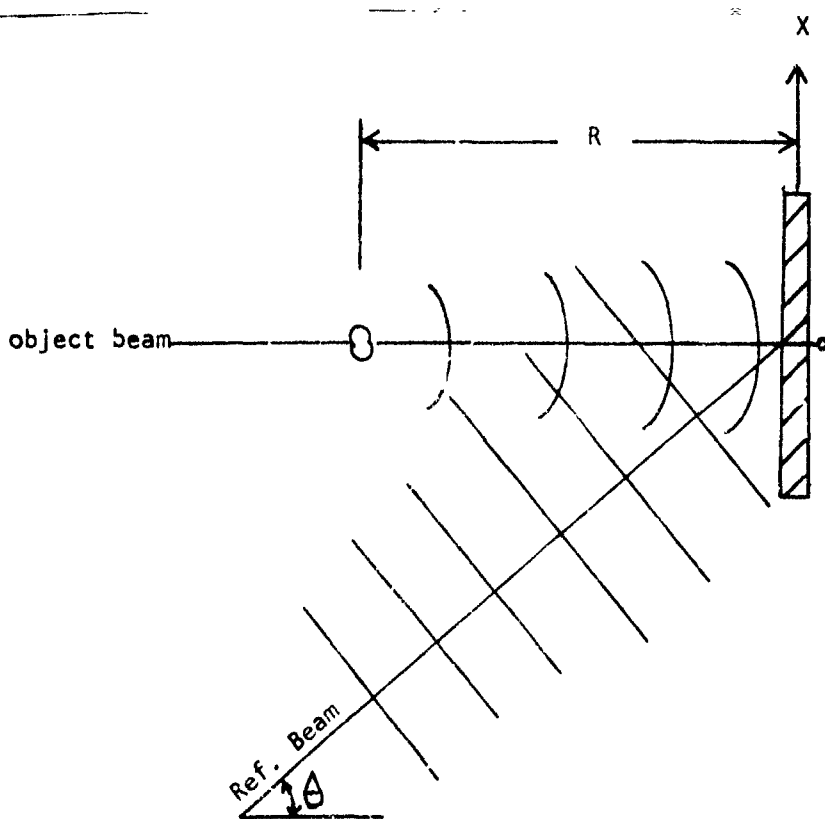


Figure 3. Recording of Off-Axis Holograms (Reference 12).

2.2.4 In the off-axis method, recording begins by splitting a parent laser beam into two spatially separated beams of different intensity. Since the reference beam acts as a carrier, this beam should be of greater intensity. Typically, the ratio of reference to object beam intensity is four to one. When the object beam passes through the scene volume, the beam is scattered as it encounters an object. This scattered wave is recorded on a special holographic plate. Simultaneously, the reference beam is

directed to the recording material without interference. Both beams must be spatially and temporally coherent as they are superimposed on the holographic plate. Once superimposed at the plate, the beams form an interference pattern. Intensity distribution is again observed as image contrast while phase information is represented by the frequency and shape of the recorded interference fringes. Following the recording process, the holographic plate is processed similar to a conventional photograph.

2.2.5 Holographic reconstruction begins by replacing the developed plate in the same orientation as existed in the recording process. Ideally, the same wavelength laser beam is passed through the exposure, but in a direction directly opposite to that observed by the reference beam during the recording process. The hologram acts as a diffraction grating. Reconstruction yields a zero order traveling wave and two additional first order diffraction waves. Higher diffraction orders are missing or quite weak since the two beam irradiance pattern is essentially sinusoidal. Of the two diffraction waves, one gives an undistorted real image in front of the hologram. The second wave gives an unwanted virtual image which is ignored. Reconstruction is illustrated in Figure 4 (Reference 12).

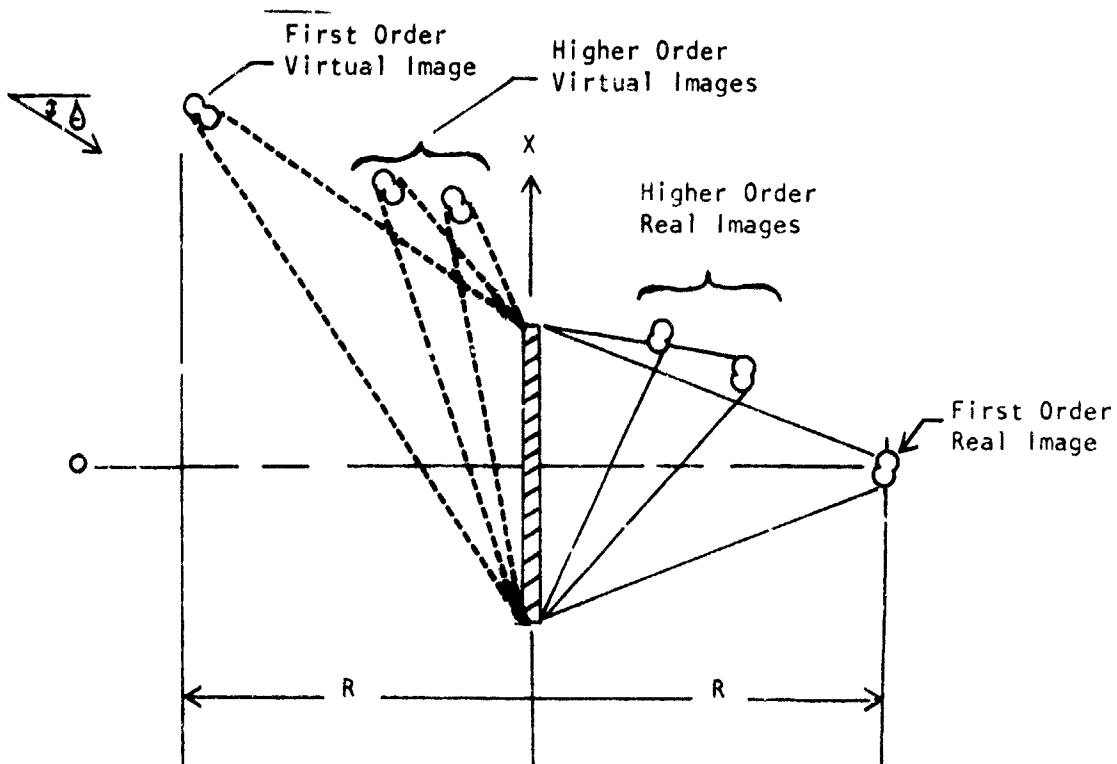


Figure 4. Reconstruction of Off-Axis Holograms (Reference 12).

2.2.6 The off-line recording method virtually eliminates self-interference between illuminated points on an object during plate exposure. In addition, the method requires less critical plate processing as well as complete spatial separation of zero and first order waves during reconstruction. Furthermore, the off-axis method reduces nonlinear effects in the recording material (Reference 13 and 14).

2.2.7 In this study, combustion holograms are recorded using diffuse illumination since direct illumination causes strong refraction patterns to be observed in the reconstructed scene (Reference 15). Diffuse illumination is introduced during the recording process by placing a screen (e.g., frosted glass) in the path of the object beam before it enters the scene volume. The diffusing screen acts to distribute radiation from points on the object over the entire plate exposure. This averaging method gives a granular texture to the reconstructed image. The observed interference is called speckle noise. As will be discussed later, speckle noise will inhibit object detection in a holographic reconstruction.

2.2.8 Particle concentration in the scene volume also is a limiting factor in holographic studies of particle laden flow fields. A high particle concentration decreases the quality of the recorded hologram due to increased wave scattering. Lower quality in the recording results in poorer particle size resolution in the reconstructed image. Several investigators (References 17 and 18) indicate that high quality holographic recordings require low particle concentrations. Witherow (Reference 18) has made an effort to quantify this concentration limit. Using holograms of monodispersed particles in silicon gel, Witherow indicates that a range of  $10^3$  to  $10^5$  particles/cm<sup>3</sup> corresponds with holographic recordings of good to poor quality respectively. These limiting values are not readily applicable to a combustion study for several obvious reasons. First, natural particle flows are rarely monodispersed. Second, in a combustion environment, other factors such as flame luminosity (Reference 15) may limit recording quality.

2.2.9 Interestingly, holography appears to share the same particle concentration limit as laser doppler. However, both methods are quite complimentary. The commonality of certain flow limitations is therefore not unexpected.

### **2.3 Holographic Image Resolution**

**2.3.1** Holography, like other optical methods, is limited in resolution by the laws of diffraction. A point source image appears as a diffraction disc whose finite dimension determines resolution. Resolution in a holographic recording is limited by the effective numerical aperture of the hologram (References 12 through 14). The numerical aperture may or may not be represented by the physical size of the exposure. Regardless, ideal resolution is never achieved due to the presence of speckle noise.

**2.3.2** As mentioned previously, speckle noise originates during the recording process when transforming direct laser illumination to diffuse illumination and is observed in the reconstructed image as a mottled scene texture. Speckle noise increases with decreasing numerical aperture in the hologram. The net effect of speckle noise is to reduce the resolving power in the hologram. Recorded objects become indistinguishable as their size approaches that of the speckle. Since speckle noise cannot be suppressed during the recording process it must be eliminated during image reconstruction.

**2.3.3** Mechanical methods of speckle removal (References 15, 21, and 22) have met with marginal success. Electronic filtering through an image analyzer has also been applied as a method for speckle removal (References 17, 18, 20, and 23). Image processing with computer software is also applicable (Reference 24). The present study chose the method employed by Briones and Wuerker (Reference 15), namely introducing a rotating mylar disc into the reconstruction apparatus.

## **3.0 EXPERIMENTAL INVESTIGATION**

### **3.1 Experiment and Application**

**3.1.1** As stated earlier, the present study used laser holography to record particle data (e.g., size and count) in the flow field above the surface of a solid propellant. The feasibility of applying holography to this combustion event was demonstrated by Briones and Wuerker (Reference 15). The intent of the present study was to restrict attention to special

propellants exhibiting parametric variations in composition. Particle size distribution for these special propellants was desired for several reasons. First, one might observe trends between propellant formulation and size distribution. If observed, such trends might assist in controlling particle size in the motor cavity through formulation. In the event trends are not observed, one can still use size distribution information to screen propellants to obtain a desired particle size. Should solid propellants exhibit characteristic "signatures" in particle size distribution, such information might be used to identify propellants showing potential stability problems. A validation in the equivalence of propellant samples through particle distribution measurement offers a potential means to maintain quality control.

3.1.2 Another possible application is in the area of solid propellant combustion modeling. Near surface particle distribution measurement provides, in essence, another boundary condition which may be of help in incorporating such effects as agglomeration into combustion models of metallized propellants. Particle distribution measurements in the flow field are a logical compliment to the chemical control studies of Miller (Reference 19).

### 3.2 Propellant Test Matrix

3.2.1 Special propellants were prepared as shown by the test matrix in Table 1. The baseline formulation was kept simple to lessen the complication of identifying potential trends between formulation and size distribution. The baseline formulation was varied parametrically to assess the influence of the following parameters on particle distribution, namely

- a. oxidizer size and distribution\*
- b. aluminum size and distribution\*
- c. HMX distribution\*

Ammonium Perchlorate and HMX samples were examined by both MSA and image analysis in an effort to characterize propellant ingredients. These results

---

\* Distribution as applied here refers to that observed in the ingredients which make up the propellant.

are also presented in Table 1. The results appear inconsistent at first glance. However, one must remember that an MSA analysis yields weight-averaged values whereas image analysis will yield number-averaged values. While one should not expect perfect agreement between the two methods, the observed discrepancies are alarming. Since the MSA analysis was consistent with a similar analysis done on the same samples prior to this study, the results from the MSA analysis will be assumed as correct. Strand burn rate measurements are summarized in Table 1. The results are consistent with the observation of Miller (Reference 19).

### 3.3 The Holography System

3.3.1 Holographic recording was conducted using a Q-switched ruby laser ( $6943\text{\AA}$ ) in conjunction with a specially constructed holocamera (Reference 15). The laser system is summarized in Table 2. Propellant combustion tests were conducted using a pre-pressurized windowed chamber to enclose a small ( $2 \times 3 \times 6\text{mm}$ ) propellant sample. Propellant ignition was implemented with a burn wire. To keep the observation windows clean, a nitrogen purge was directed around the propellant sample during combustion tests. Recording functions (i.e., propellant ignition, laser discharge, chamber vent) were sequenced through a mechanical timer. Time delays must be set manually and were determined by trial and error. One can expect the timer settings to vary in relation to the varying burn rate of different propellants. Figure 5 shows the layout of the recording area.

3.3.2 A spectra Physics Model 175 continuous wave helium neon laser ( $6389\text{\AA}$ ) was used to provide illumination during holographic reconstruction. Reconstruction was conducted in a separate area using the layout shown in Figure 6. The procedure begins by replacing the developed hologram back into a portable lens box unit of the holocamera. The lens box allows one to maintain the same optical arrangement as was used during recording. Once placed into the lens box, the hoiographic plate cannot itself be re-positioned. Therefore, the lens box is placed upon a specially constructed pedestal which allows the plate to be positioned for optimum illumination and resolution. The pedestal, which incorporates three axis positioning, leveling, and tilt control is shown in Figure 7.

Table 1: LASER SPECIFICATIONS

<u>Type</u>	<u>Recording</u>	<u>Reconstruction</u>
	<u>Pulsed Ruby</u>	<u>Helium Neon</u>
wavelength	6943 Å	6389 Å
Average Output Power (Energy)	1 Joule	50 mw.
Raw Beam Diameter ( $d_b$ )	2.0 mm.	2.0 mm.
Beam Divergence	0.007 mv.	.007 mv.
Ocular SEED* ( $d_b < d_p$ )	$2.26 \times 10^5$ cm.	$2.8 \times 10^3$ cm.
Ocular Optical Density	6.72	1.7
Exposure Duration	$5 \times 10^{-8}$ sec. $1 \times 10^{-8}$ sec.	.25 sec.
Laser Pulse Duration	50 ns. (single & double) (pulse ) 10 ns. (single pulse ) (chopped )	continuous
Safety Eyewear	American Optical #585 O.D. = 46	American Optical #581 O.D. = 6.0

\* SEED = Safe Eye Exposure Distance

$d_p$  = pupil diameter, assumed at 7mm

Table 2: PROPELLANT TEST MATRIX

	Series A					Series B					Series C					
Designation	1	4	5	9	10	11	15	17	18	20	21	23	32	34	35	37
% TPB	15	15	15	15	15	15	14.4	14.4	14.4	14.4	14.4	14.4	14.4	14.4	14.4	14.4
% A <sub>1</sub>	55	55	30	43	55	53.5	53.5	49.3	49.3	43	43	31	31	43	43	43
200 $\mu\text{m}$																
200 $\mu\text{m}$																
50 $\mu\text{m}$																
20 $\mu\text{m}$																
6 $\mu\text{m}$																
% Al																
90 $\mu\text{m}$																
6 $\mu\text{m}$																
% HMX																
Class E																
$\dot{r}$ (in/sec)	.313	.300	.320	.325	.307	.260	.283	.263	.238	.246	.190	.213	.269	.297	.213	.263
@ 68 atm																
index = n	.583	.390	.586	.613	.421	.425	.592	.453	.527	.502	.447	.369	.354	.476	.339	.351
MSA Analysis (Mean Particle Size)																
AP = 418, 185, 34, 21, and 6.9 $\mu\text{m}$																
HMX = 5.3 $\mu\text{m}$																
Image Analysis (Mean Particle Size)																
AP = 418, 185, 70, 36, and 21.5 $\mu\text{m}$																
HMX = 7.2 $\mu\text{m}$																

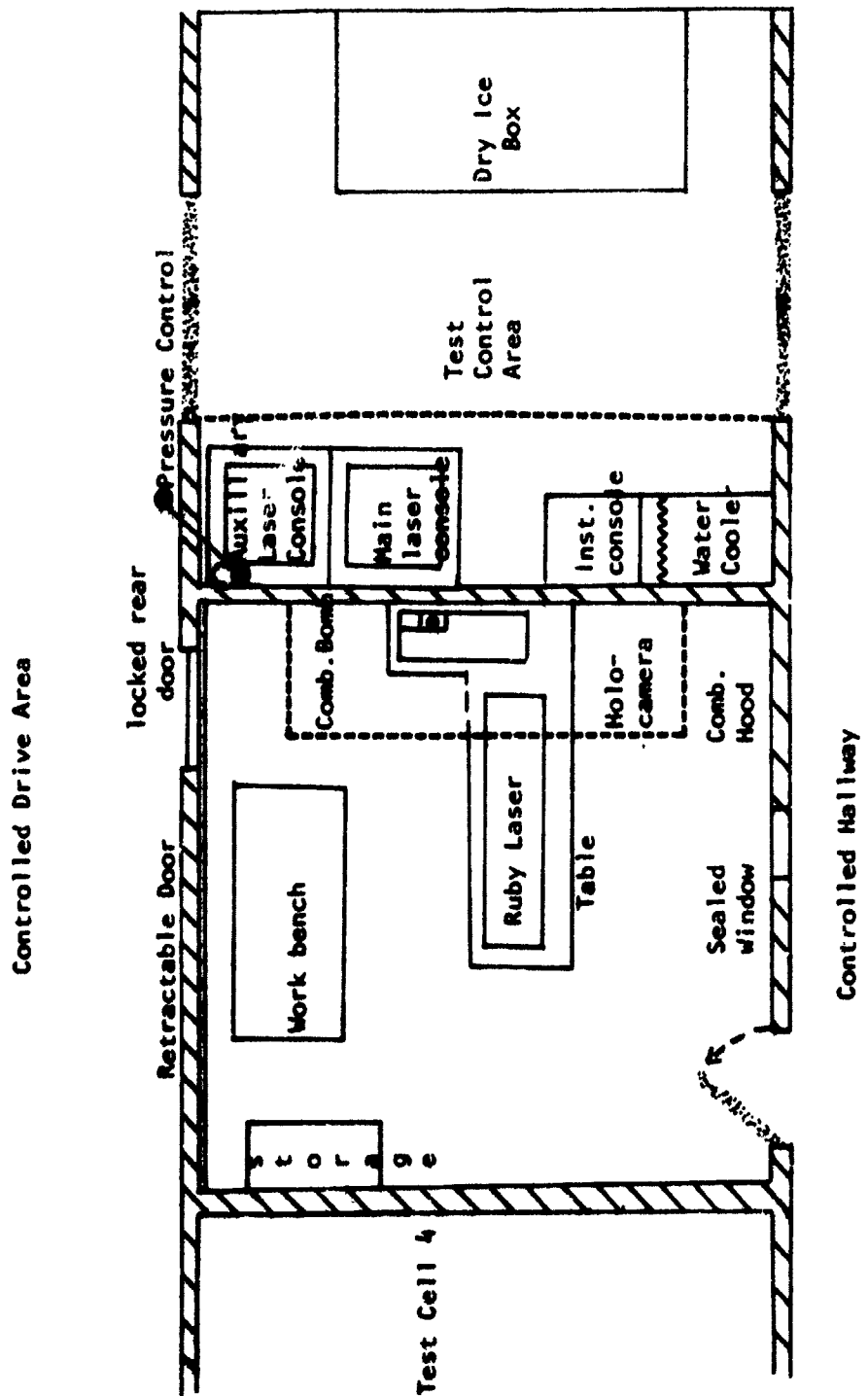


Figure 5. Layout of Recording Area

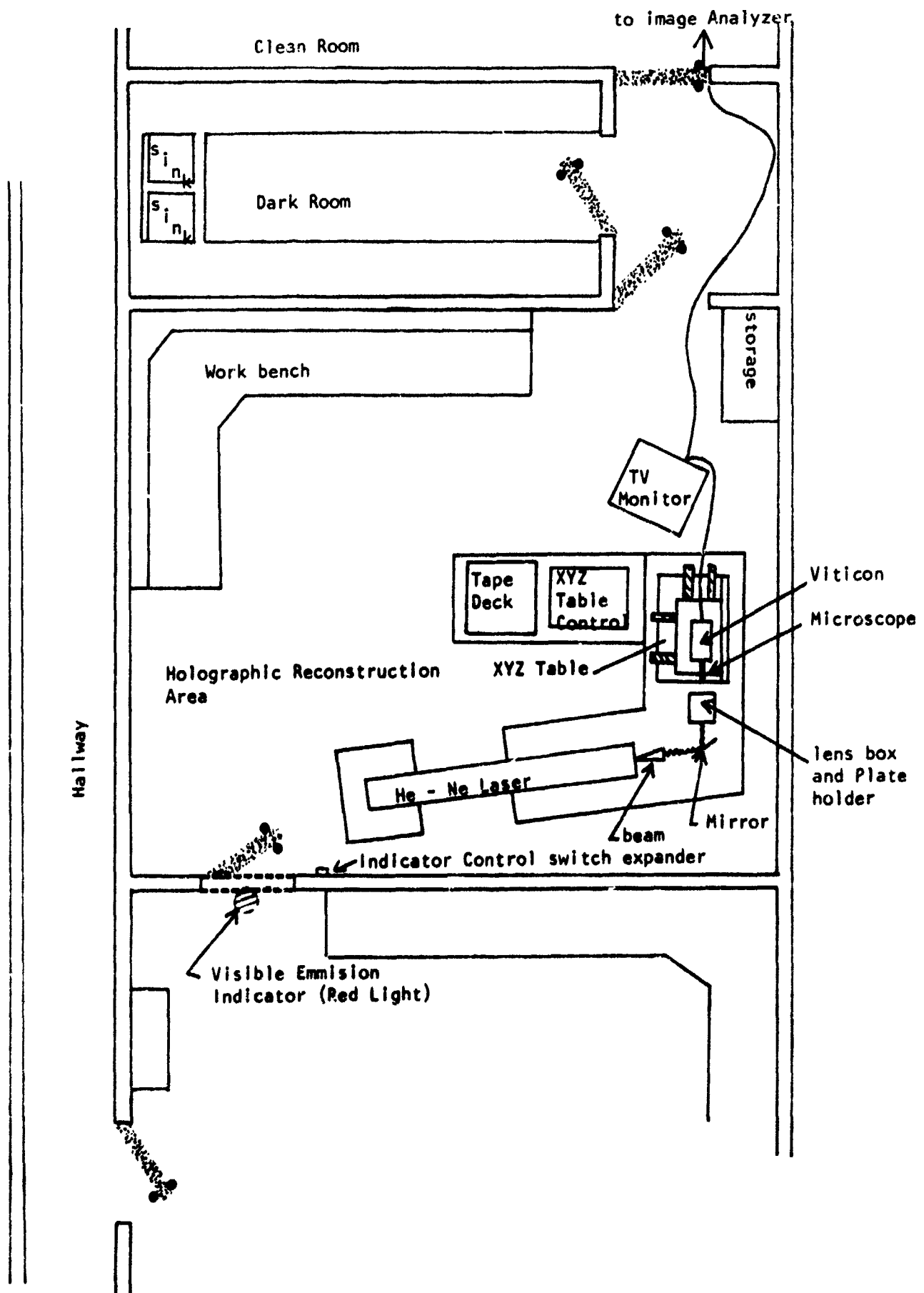


Figure 6. Layout of Reconstruction Area.

3.3.3 The constructed image is received through a conventional microscope. The microscope is in turn attached to a vidicon camera. The camera incorporates a silicon-faced tube which is sensitive to red light. Video output from the camera is passed to either a standard television monitor or a Bausch and Lomb Omnicon image analyzer. A video monitor is required to establish the focus and magnification in the imaging system. The electronic image analyzer supplies an automated data retrieval capability with regard to particle size and count information.

#### 4.0 EXPERIMENTAL PROCEDURES

##### 4.1 Image Interrogation

4.1.1 As shown in Figure 8, the reconstructed scene volume of the combustion field is divided into smaller subvolumes whose cross section is defined at any point along the optical axis by the overall magnification of the imaging system. Bexon (Reference 20) has shown that the overall magnification of an imaging system of the type used in this study will change slightly in each plane along the optical axis. Fortunately, these incremental changes in magnification can be calculated by knowing the magnification in a predetermined reference plane and the separation distance between the reference plane to the adjacent plane of interest along the optical axis. One establishes a reference plane by placing a known target in the scene volume during the recording of the hologram. Upon reconstruction, the known target is used to calibrate the overall magnification in the reference plane. The location of the reference plane is specified by the position of optimum focus on the target. Once established, this position represents the relative zero location along the optical axis. All subsequent movements along the optical axis are made with reference to this zero position.

4.1.2 Several points should be made at this time. First, in this study, each plane along the optical axis will present an image containing both in and out of focus particles. The focus of the imaging system should not be changed once established in the reference plane. Therefore, there is a need to develop some criteria by which to identify out of focus particles. This requirement will be explained in more detail later. Second,

since the location of the reference plane is a relative position, this location must be reset for each hologram. Third, the overall magnification at points along the optical axis must be determined in order to prevent redundant particle sizing when examining adjacent subvolumes.

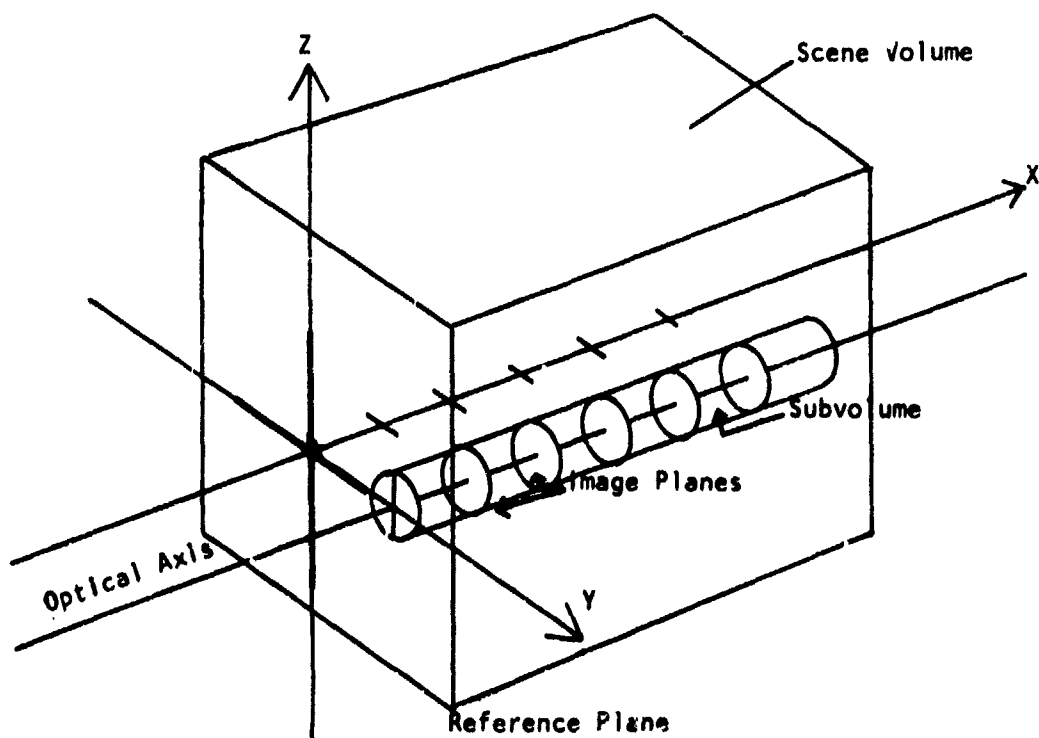


Figure 8. Scene Interrogation

4.1.3 A total screening of the entire reconstructed scene, though desired for completeness, may not be required to obtain a statistical average which can represent the actual particle distribution above the burning propellant surface. The total number of particles which one must count is dependent upon both the extent of isotropy\* in the particle field and degree of particle dispersion. Obviously, a monodispersed particle field which is totally isotropic does not require a large particle count. Polydispersed particle fields present a greater problem. A possible solution is to count particles until some chosen statistical average shows little change with increasing particle count (Reference 8). This condition

\* In an isotropic combustion field, particle concentration is invariant in all directions.

is observed by plotting mean values against particle count. This proposed method is not foolproof since its success assumes that particles are randomly distributed such that the final mean value reflects the proper weighting in all particle sizes. A cursory interrogation of the entire scene volume may be required to lend support to statistical determinations.

4.1.4 The results reported by Briones and Wuerker (Reference 15) appear to indicate that the particle field above a burning solid propellant does not show any layering as to particle size. However, this observation is based on a particle count of 568 particles in one small region ( $6.4 \times 10^{-4} \text{ cm}^3$ ) above the propellant surface. Furthermore, these results were obtained from one hologram and hence represent a single test of one propellant sample (16% Al, 84%  $A_p$ ). Admittedly, it is somewhat premature to predict isotropic behavior in solid propellant combustion particle fields based upon this single observation. However, this study proceeded using an isotropic assumption. The isotropic assumption can be checked visually or by comparing statistical averages of particle distribution as determined for discrete layers from the optical axis. If an isotropic assumption is not applicable, spatial coordinates must be assigned to the particles which are counted. This indexing procedure would allow direct monitoring of any spatial variation in mean particle size. Since solid propellant combustion is essentially a steady state process, the particle field is assumed to equilibrate quickly with regard to its mean properties. Therefore, mean properties are assumed to have no temporal dependence. This assumption can be validated by examining mean particle properties at different times into the propellant burn. This task is accomplished during the recording process by double pulsing the illuminating laser. The reference beam polarity is flipped on the second pulse. The overall process gives two distinct holograms which represent two burn times (References 15 and 16). Using the equipment described in section 3.0, the interval between the two recordings can range from 5 to 500  $\mu\text{sec}$ .

4.1.5 As mentioned earlier, the combustion window bomb utilizes a nitrogen purge during the propellant burn. Turbulent mixing between the purge gas and the products of combustion will occur. The influence of

the purge gas diminished near the propellant surface. Since interest lies only in particle distribution associated with propellant combustion, sampling will be restricted to small distances from the propellant surface.

#### 4.2 Particle Recognition

4.2.1 Sizing particles in the reconstructed combustion field begins with particle recognition. The most immediate means by which to identify particles is to use the human eye. Consider briefly how this complex process of object recognition proceeds. The eye receives a visual input. Sensory information is passed to the brain for processing. For example, background noise or other features of noninterest are automatically subtracted from the image. Compensation is made for uneven illumination. As an image is received, the eye integrates over the total area of the scene. One "sees" continuous tone images where colors blend in intensity (level) and spatially (area). Detected features are examined with regard to shape, focus, and contrast. Object boundaries are distinguished by discernable contrast with the surrounding media. Once appropriate boundaries have been defined, an object can be sized. Objects are sized individually by comparing the object to a calibrated reference. In a combustion field where there are many objects, manual sizing becomes a long and tedious operation. Furthermore, the human eye can tire and is also subject to false images (optical illusions). For holographically examining particles in a combustion flow field, one realizes that automated particle detection and sizing is a more practical approach.

4.2.2 Automation is a universal term which has varying degrees of interpretation. As applied to the discussion which follows, automated particle data retrieval refers to the decomposing of an image plane into a video signal for subsequent processing by a computer and/or other electronic devices. At this point, a distinction is drawn between electronic versus computer image analysis. Electronic image analysis evolves from an analog process and involves only the direct acquisition of image data. Computer image analysis involves the digitization of an image (acquisition) for subsequent analysis by computer software (processing) (References 25 and 26).

4.2.3 As stated earlier, objects are detected in an image using discernable contrast. Discernable contrast is quantized by discrete grey levels. Hence, contrast is measured according to the grey level sensitivity of the image receiver. For example, a scanning microdensitometer can detect 256 levels of grey. A good photographic film can record about 200 of these levels. The human eye can resolve about 50 grey levels while an electronic image analyzer works with 40 levels. Thus, electronic detection by discernable contrast is ideally as good or slightly poorer than the capability exhibited by the human eye. If an object cannot be detected by the eye, it will probably resist detection by an electronic image analyzer. However, electronic analyzers offer a major advantage. Detected objects are sized virtually instantaneously. Hence, a field of polydispersed particles can be examined much faster than can be achieved manually. Furthermore, if properly calibrated, these machines offer greater accuracy since they are not subject to fatigue.

#### 4.3 Electronic Image Analysis

4.3.1 A typical electronic image analyzer operates in the following manner (References 28 and 29). An image is brought to the face of a vidicon tube by a lens arrangement. An electronic beam scans the face of the tube much like one sweeps across a page of printed text. The output voltage from the vidicon tube varies with the brightness of the image. Thus, as the beam travels horizontally across a line (raster) on the tube face, brightness variations are observed electronically as a voltage time waveform. Scanning motion is from left to right. As the beam is returned to a new starting position, the line of travel is blanked so that detection is only in the forward (left to right) direction. The scan procedure is therefore interlaced.\* The beam initially sweeps every other line and then returns to pick up those lines neglected during the initial sweep. Vertical sampling can also be added. The reader is referred to Reference 27 for more details.

---

\* Some machines, for example the Imanco Quantinet image analyzer, employ a slower sequential line scan procedure.

4.3.2 A silicon vidicon tube which has  $m$  lines of total scan and  $n$  light values per line has a total of  $N = m \cdot n$  picture elements (pixels). A standard tube contains  $2.5 \times 10^5$  pixels ( $m = 512$ ,  $n = 480$ ). The total scan period associated with such a tube is approximately 0.1 sec. A silicon vidicon tube is used in the present study since it shows excellent spectral response and sensitivity to wavelengths in the red regime (Reference 27). In contrast, the human eye shows poorer spectral response in this regime.

4.3.3 From the previous remarks, it is obvious that grey level information is carried in the voltage signal from vidicon. Grey level information, as applied to electronic object detection, is used as shown in Figure 9 (Reference 30). The amplitude of the voltage signal from the vidicon is compared to a preset reference value. When the amplitude of the input signal rises above that of the reference value, a binary signal is switched to a logical "1". When the amplitude falls below that of the reference, the binary signal returns to logical "0". The duration of the binary pulse corresponds to the size of the object along the line of scan.

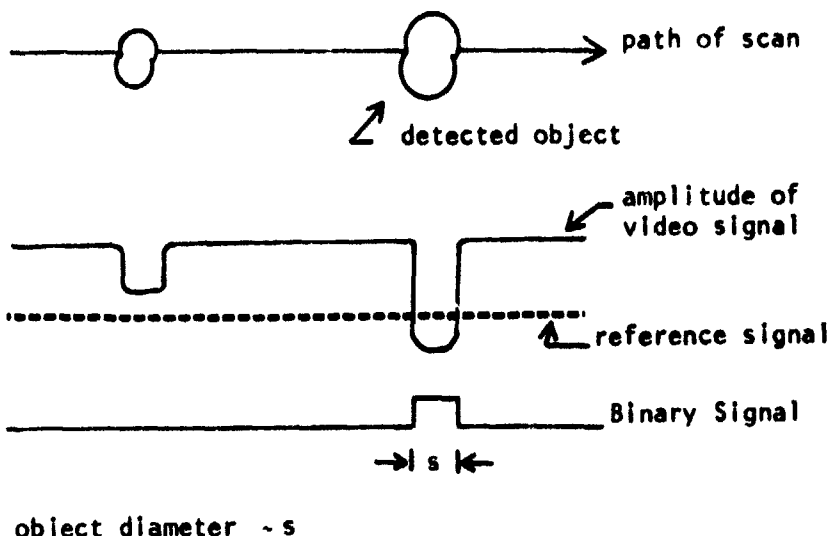


Figure 9. Electronic Particle Detection and Sizing (Reference 30).

4.3.4 There are problems associated with electronic object detection. First, non-spherical objects of similar reflectance can produce different vidicon signal variations depending upon the position of the object. Since detection proceeds from a fixed reference, position dependent intensity variations can lead to false detection or no detection at all. This argument can also be extended to include focus problems when working with images showing an extended depth of field. Secondly, optical devices, such as microscopes or camera lenses, suffer from light fall-off along the edges of the field of view. This aperture effect reduces the dynamic range\* of the image receiver. Similarly, glare or uneven illumination can also reduce such sensitivity.

4.3.5 Several electronic image analyzers have been used in holographic particle studies (References 17, 18, 20, 23, and 31). The present study elected to use the Bausch and Lomb Pattern Analysis System. The decision to use this system was based solely on the basis of its on site availability.

## 5.0 RESULTS AND DISCUSSION

### 5.1 Initial Investigations

5.1.1 Holograms of an AF 1951 resolution target were recorded using the helium neon laser and holocamera discussed in section 3.3. These holograms were taken to verify holocamera operation and to provide holograms for evaluating size resolution limits in the proposed automated data retrieval system. The holograms showed a size resolution of approximately  $10\mu\text{m}$  when examined visually via a video monitor. Resolution would be worse for combustion holograms since for those holograms there is a slight difference in the wavelength between the recording and reconstruction laser.

5.1.2 A second set of holograms was recorded also using the helium neon laser. The target was a half inch thick acrylic disc which contained dispersed aluminum oxide particles ( $d \sim 10\mu\text{m}$ ). These holograms were to be used to investigate problems associated with discriminating in and out of

---

\* Dynamic range is defined as the ratio of maximum input signal to the minimum detectable signal.

focus particles using an electronic image analyzer. Unfortunately, the acrylic holding material was too crystalline in its internal structure with the result that the recorded holograms exhibit severe refraction upon their reconstruction. No further effort was made to substitute a new holding material since experiments using holograms of the resolution target showed detection was inhibited for objects much larger than the particles in the disc. Since size resolution could not be improved in the data retrieval system, the problem of out of focus particles was at this point of secondary importance to this study.

## 5.2 Combustion Holograms

5.2.1 A test facility was constructed to record combustion holograms of the propellants described in section 3.2. Attempts to record these holograms were not successful due to unexplained fogging of the photographic plates. A series of experiments were conducted to identify the cause of the plate fogging.

5.2.2 Flame light from the combustion of the propellant was eliminated as a possible source of interference. First, the narrow band filter was in place during all attempts to record propellant combustion. Second, plate fogging was also observed when attempting to record holograms of inert objects.

5.2.3 The internal alignment of the pulsed ruby laser being used during recording was rechecked and found to be satisfactory. However, it was suggested that the ruby laser was placed too close to the holocamera during recording. Since the ruby rods become transparent during lasing, it was suspected that the intense light from the flash lamps which surround the rods was being transmitted to the photographic plate. Therefore, the laser was reversed from the holocamera with the source beam now being transmitted to the camera by mirrors. The optical path length ( $L$ ) to the camera was now increased by a factor of ten or more. Since the light intensity from the lamps would decrease as  $1/L^2$ , any interference from the lamps would be virtually eliminated. However, plate fogging was still observed.

5.2.4 Another possible answer to plate fogging was improper alignment of the reflecting surfaces in the holocamera. It was observed that internal alignment of the holocamera was sensitive to any movement of the camera housing. Mirror mounts were occasionally discovered to be loose. Unfortunately, since the lens box had to be removed to perform holographic reconstructions, the camera alignment had to be constantly re-established. Once the internal alignment had been set, the ratio of object to reference beam intensity was checked visually and found to be satisfactory. Even when alignment in the holocamera was carefully preserved, plate fogging continued.

5.2.5 The holocamera housing was checked for possible leakage from outside light. The camera was loaded and subjected to room illumination. Subsequent development of the plate revealed no plate exposure thus verifying the integrity of the camera housing.

5.2.6 The problem of plate fogging was never resolved though the facts lead one to suspect that the holocamera is still misaligned. Holograms were taken with the holocamera during recording with the helium neon laser. The ruby laser was repositioned to eliminate flash lamp interference. The intensity ratio between the object and reference beams was checked and verified as satisfactory. The holocamera housing was checked for light leakage, and none was found. Holographic plates were fogged regardless of the target being recorded. The alignment of the holocamera was found to be sensitive to movements of the holocamera housing, such as occurs when the lens box is removed. Problems with the proposed automated data retrieval system obviated any need in this study to continue attempts to make combustion holograms.

### 5.3 Positioning

5.3.1 Accurate positioning is an integral part of the scene interrogation process proposed in section 4.1. The viewer must be aware of both

his position within the total scene and the area covered by his field of view. This information is required to prevent redundant particle counts. Originally, the microscope-camera arrangement was mounted on a movable (X-Y-Z) platform. The platform had a minimum step increment of 40 $\mu$ m along each axis. Coordinate information on the platform was relayed to the operator by a digital display. The holographic plate was held stationary and the entire exposure illuminated by a fixed laser source. Subvolumes, as defined by the imaging system, were indexed and scanned using the moving platform.

5.3.2 Several problems caused the above positioning arrangement to be abandoned. First, the step increments of the platform were much too coarse for accurate positioning. Second, the platform was subject to drift. A fixed position within the scene volume was difficult to maintain for a period sufficient to make an accurate particle count since drift occurred in 40 $\mu$ m increments, i.e., the minimum step accuracy. Third, a requirement for higher magnification was accompanied by an additional requirement of more illumination to the field of view. To meet this demand, the illuminating laser beam was collimated to a smaller diameter during reconstruction. This action results in a smaller illuminated region on the exposure. Because the laser source remained fixed, lateral plate movement was required to examine all areas over the exposure. Since beam collimation necessitates movement of the plate, it was decided to also fix the location of the camera and interrogate the scene volume by moving the holographic plate along the optical axis. Plate movement was accomplished using the lens box pedestal described in Section 3.3. The minimum step increments were reduced to 10 $\mu$ m. More accurate manual positioning devices with step increments of 1 $\mu$ m are available commercially, but were not obtained for this study.

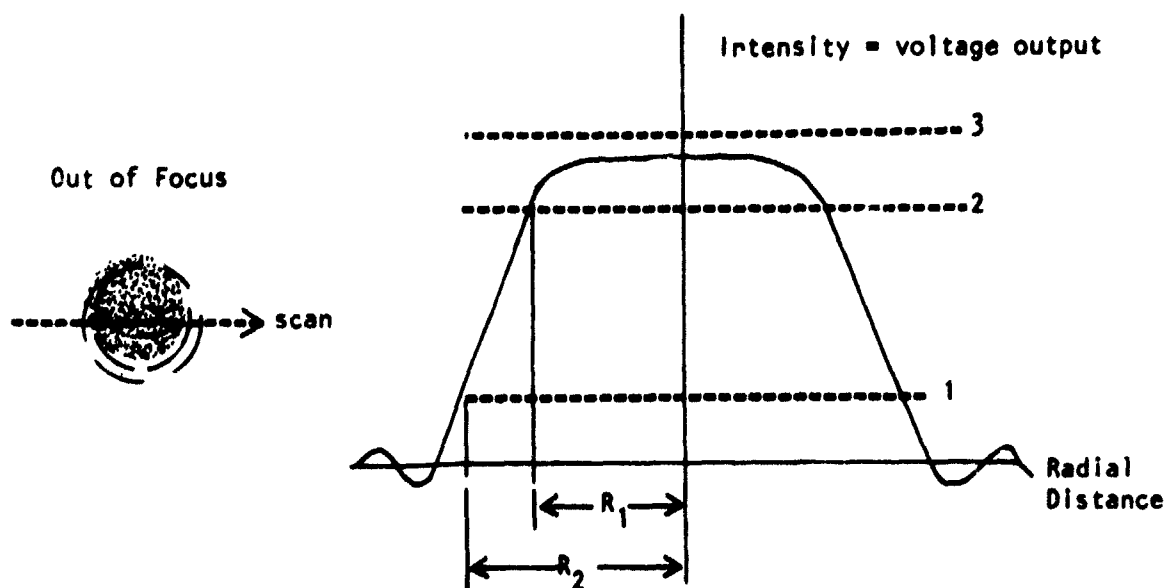
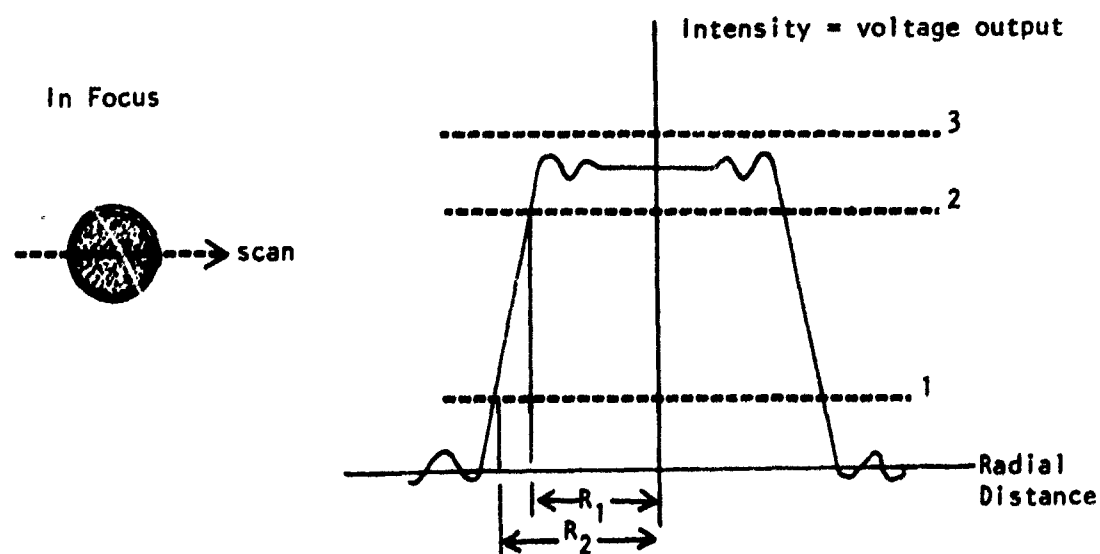
5.3.3 The imaging system exhibited a size resolution of approximately 10 $\mu$ m. Electronic object detection using the image analyzer was limited to a resolution of about 50 $\mu$ m. A shading corrector was purchased to improve the performance of the image analyzer. However, the unit was defective and was not available for this study. Detection could be expected to improve with shading correction.

## 5.4 Particle Focus

5.4.1 As stated earlier, any image plane within the reconstructed volume of the combustion holograms examined in this study shows both in and out of focus particles. Obviously, out of focus particles must be screened from detection. Screening requires either a definition of focus in terms of the voltage output to the electronic image analyzer or manual judgement.

5.4.2 Consider first the process of manual focus determination. One observes marked changes in edge contrast in a particle when passing through the position of optimum focus with the imaging system. The initial reaction to such an observation is to use grey level information to define focus. Electronically, the procedure involves specifying an acceptable voltage rise in the output signal from the vidicon. As illustrated in Figure 10, the voltage output (intensity) between two reference levels will steepen as a particle comes into focus. Bexon (References 20 and 31) monitors individual particle area measurements at two threshold levels to determine particle focus. Trolinger (Reference 23) employs a similar procedure, but uses particle measurements of area and perimeter. Both schemes work reasonably well but require that information be cataloged on each detected particle. This requirement demands that individual particles be assigned spatial coordinates to facilitate monitoring of stored information. Since the Bausch and Lomb system cannot index individual particles, these focus algorithms cannot be used. A different method of focus determination is required for this study.

5.4.3 An immediate option was to discriminate particle focus manually using a light pen. This idea was rejected for several reasons. First, such a procedure defeats the purpose of applying electronic image analysis, namely speed in data retrieval. Second, manual focus discrimination for small particles requires very fine step control ( $<10\mu\text{m}$ ). Visual interpretations are also biased by operator error.



Focus:  $R_2 - R_1 \sim 0$

Figure 10. Focus Criteria (Reference 23).

5.4.4 A second option was to establish the focus criteria using the previously mentioned target in the reference plane. Once the focus is manually established in this plane, all detected particles from this plane are assumed to be in focus. This focus criteria proved to be inadequate for several reasons. Since speckle noise interferes with the detection of smaller objects, a focus criteria established through grey level thresholding with larger objects does not hold when applied to smaller objects where edge contrast diminishes. Changes in illumination from that observed in the reference plane also compromises object detection and hence focus determination.

5.4.5 Thus, as shown by other investigators (References 17, 18, 20, 21, and 23), electronic image analysis of a holographic reconstruction of a particle field requires: a) complete spatial indexing of detected features, b) computer software to monitor information on detected features, and c) good holographic reconstructions exhibiting both low optical noise and good illumination in all image planes.

## 6.0 CONCLUSIONS AND RECOMMENDATIONS

### 6.1 Conclusions

6.1.1 Automated data retrieval from holographic reconstructions represents a key requirement in performing the experiment proposed earlier. A statistical representation of particle size distribution, as sought by this study, requires a sufficiently large particle count to assure confidence in any proposed correlations. The large amount of data required for such assurance rules out manual data retrieval. For example, Briones and Wuerker report a work period of eight days to count 568 particles in one small region of one holographic reconstruction. Obviously, any proposed statistical representation of the particle field above a burning solid propellant must be based on a much larger particle count and verified with several holograms. Practicality dictates turning to some form of automated particle sizing and counting procedure when dealing with holographic reconstructions of particle flow fields.

6.1.2 One approach to automated data retrieval is to use an electronic image analyzer to size and count particles in the holographic reconstruction of the particle field. Given sufficient object contrast in the reconstructed scene, an electronic image analyzer will perform adequately. However, as discussed earlier, holographic reconstructions of small ( $<50\mu\text{m}$ ) objects show limited contrast and poor edge definition. Though discernable with the human eye, such objects are not readily detected by an electronic analyzer. Electronic image analysis examines measured intensity and grey levels against preset reference values to detect and size objects. As expected, both operations are inhibited for objects showing poor edge definition and contrast.

6.1.3 Each image plane in a reconstructed hologram of a particle field includes objects which are both in and out of focus. The present study reinforces the findings of other investigations (References 20, 23, and 31), namely that focus discrimination requires a complete spatial indexing of all detected features. Once features have been indexed, detected objects can be monitored individually to determine status with regard to focus. Only data on focused particles is stored for inclusion in a statistical analysis. The reported success of focus algorithms is encouraging (References 17, 23, and 31).

6.1.4 The degree of success in applying electronic image analysis to holographic reconstructions seems to be based primarily upon (a) the type of machine (analyzer) being used, (b) the quality of the holographic reconstruction, (c) the properties associated with the recorded event, such as particle concentration, and (d) the dynamic range associated with the system receiving the reconstructed image.

## 6.2 Recommendations

6.2.1 The factor which limits the application of electronic image analysis to examine holographic reconstructions of particle fields is the quality of the recorded image. One seeks methods which will improve image quality. Image improvement during recording is limited since the process

is primarily dependent upon the equipment being used and the skill of the operator. Image quality can also be influenced by plate development. Care must be exercised during this procedure. Even with adequate provisions being taken during recording and plate development, one must still contend with optical noise.

6.2.2 Optical noise is suppressed during the reconstruction process. One can regard out of focus particles as optical noise since such features are to be neglected in any particle count. An approach to feature detection against a noisy background involves optical (analog) filtering (References 32 and 33). These filters are real-time devices which would ideally provide an image with objects representing a prespecified size range and shape. Such filters have been used successfully in airborne reconnaissance. Pattern detection has been used extensively in radar imaging. As applied to the present problem, analog filters would be constructed to provide feature detection in various size range intervals. In principle, analog filters could be used to assist an electronic image analyzer in its task of detection. However, optical filters must still contend with problems such as out of focus particles.

6.2.3 Another approach to noise suppression is to apply computer image processing. A thorough discussion of image processing can be found in the book by Pratt (Reference 26). Basically, once a picture frame (i.e., image plane) is digitized, it can be altered using computer software to manipulate grey level information. For example, image enhancement has been used in sizing particles from electron microscope images (Reference 34). Computer enhancement has proven effective in improving image quality originally lost by high magnification or photographic limitations (References 35 through 38). More recently, computer methods have been applied to improve the image quality of holographic reconstructions of spray droplet fields (Reference 24). The strength of image processing lies in its flexibility in selectively improving image quality. The obvious weakness of such an approach is that computer image processing takes considerable time and data manipulation to implement as compared to electronic image analysis. One desires the best of both worlds, namely the speed of electronic image analysis and the versatility provided by computer software.

6.2.4 The marriage of both methods is already a reality (References 39 and 40). The technology in image analysis is advancing far too rapidly to capture and summarize the area in this report. Undoubtedly, many of the obstacles encountered in this study with regards to data retrieval will be overcome as new hardware is developed. The reader should therefore be cautioned against premature judgement against electronic image analysis of holograms. Naturally, there exist unique problems to be solved, yet the investigations which seek solutions to those problems are only just beginning.

#### REFERENCES

1. Dobbins, R.A. and Temkin, S., "Measurement of Particulate Acoustic Attenuation," AIAA J., V.2, No. 6, June 1964.
2. Temkin, S. and Dobbin, R.A., "Attenuation and Dispersion of Sound by Particulate Relaxation Processes," J. Acoust. Soc. Amer., V. 40, No. 2, February 1966.
3. Levine, J.N. and Cullick, F.E.C., "Nonlinear Analysis of Solid Rocket Combustion Instability, Vol. 1: Analysis and Results," AFRPL-TR-74-45, July 1974.
4. Lovine, R.L., "Standardized Stability Prediction Method for Solid Rocket Motors, Vol. 1," AFRPL-TR-76-32, May 1976.
5. Coats, D.E., et. al., "A Computer Program for the Prediction of Solid Propellant Rocket Motor Performance, Vol. 1," AFRPL-TR-75-36, July 1975.
6. Soo, S.L., Fluid Dynamics of Multiphase Systems, Blaisdell Publishing Co., 1967.
7. Riyad, R.I. and Clayton, F.C., Particle Size: Measurement, Interpretation, and Application, John Wiley and Sons, Inc., 1963.
8. Hesketh, H.E., Fine Particles In Gaseous Media, Ann Arbor Science Publishers, Inc., 1977.
9. Buchava, P., et. al., The Accuracy of Flow Measurements by Laser Doppler Methods, Proceedings of the LDA Symposium Copenhagen, Hemisphere Publishing Corporation, June 1976.
10. "Capabilities in Laser Instrumentation," SDL Report No. 75-6019, Spectron Development Laboratories, Inc., October 1975.
11. Durst, F. and Eliasson, B., "Properties of Laser Doppler Signals and their Exploitation for Particle Size Measurements," Proceedings of the LDA Symposium Copenhagen, June 1976.
12. Yu, F.T.S., Introduction to Diffraction, Information Processing, and Holography, MIT Press, 1973.

13. Smith, H.M., Principles of Holography, 2nd Edition, Wiley Interscience 1975.
14. Ostrovsky, Y.I., Holography and Its Applications, MIR Publishers, Moscow, 1977.
15. Briones, R.A., and Wuerker, R.F., "Application of Holography to the Combustion Characterization of Solid Rocket Propellants," AFRPL-TR-77-90, April 1978.
16. Krile, T.F., et. al., "Holographic Representations of Space-Variant Systems Using Phase-Coded Reference Beams," Applied Optics, V. 16, No. 12, December 1977.
17. Belz, R.A., and Menzel, R.W., "Particle Field Holography at Arnold Engineering Development Center," Optical Engineering, V. 1, No. 3, May-June 1979.
18. Witherow, W.K., "A High Resolution Holographic Particle Sizing System," Optical Engineering, V. 1, No. 3, May-June 1979.
19. Miller, R.R., et. al., "Control of Solids Distribution in HTPB Propellants," AFRPL-TR-78-14, April 1978.
20. Bexon, R., "Magnification in Aerosol Sizing by Holography," J. Phys. E. Sci. Instrum., Vol. 6, 1973.
21. Ih, C.S., and Baxter, L.A., "Improved Random Spatial Phase Modulations for Speckle Elimination," Applied Optics, V. 17, No. 9, May 1978.
22. Cox, M.E., and Vahala, K.J., "Image Plume Holograms for Holographic Microscopy," Applied Optics, V. 17, No. 9, May 1978.
23. Trolinger, J.D., "An Examination of Automatic Data Reduction Methods for Particle Field Holograms," SDL Report No. 77-6230, Spectron Development Laboratories, Inc., December 1977.
24. Feinstein, S.P., and Girard, M.A., "Feasibility of Automated Dropsize Distributions from Holographic Data Using Digital Image Processing Techniques," 17th Aerospace Sciences Meeting, Paper No. 79-0297, January 1979.
25. Computer Eye Handbook, Spatial Data Systems, Inc., Second Edition, 1974.
26. Pratt, W.K., Digital Image Processing, Wiley Interscience, 1978.
27. Eye Com Picture Digitizer and Display, Spatial Data System, Inc., First Edition, 1977.
28. Dyall, W.T., "Televiewers: What Do You Mean by High Resolution," Electro-Optical Systems Design, March 1978.
29. Sparks, J.E., "Television that Nobody Watches," Machine Design, February 10, 1972.
30. Shear, R., "Effects of Shading in Images," Electro-Optical Systems Design, February 1978.

31. Bexon, R., Bishop, G.D., and Gibbs, J., "Aerosol Sizing by Holography Using the Quantimet," IMANCO Report on Equipment and Applications, No. 3.
32. Casasent, D., "Optical Data Processing for Engineers, Part 1: Fundamentals, Techniques and System Architectures," Electro-Optical Systems Design, February 1978.
33. Casasent, D., "Optical Data Processing for Engineers, Part 2: Real Time Devices," Electro-Optical Systems Design, April 1978.
34. Hall, E.L., Varsi, G., Thompson, W.B. and Gauldin, R., "Computer Measurement of Particle Sizes in Electron Microscope Images," IEEE Transactions on Systems, Man, and Cybernetics, February 1976.
35. Naderi, F., and Sawchuk, A.A., "Detection of Low Contrast Images in Film-Grain Noise," Applied Optics, V. 17, No. 18, September 1978.
36. Cannare, T.M., Trussel, H.J., and Hunt, B.R., "Comparison of Image Restoration Methods," Applied Optics, V. 17, No. 21, November 1978.
37. Matuska, W., et. al., "Enhancement of Solar Corona and Comet Details," Optical Engineering, V. 17, No. 6, November-December 1978.
38. Mengers, P., "Low Contrast Imaging," Electro-Optical Systems Design, October 1978.
39. Toner, M.C., Dix, M.J., and Sawistowski, H., "Automatic Image Analyser," Microprocessors, V. 2, No. 2, April 1978.
40. Toner, M.C., Dix, M.J., and Sawistowski, H., "A Television-Microprocessor System for High Speed Image Analysis," J. Phys. E: Instrum., V. 11, 1978.